MeV sterile neutrino in light of the Cabibbo-angle anomaly

Teppei Kitahara[1,2,*] and Kohsaku Tobioka[3,4,†]

[1]*CAS Key Laboratory of Theoretical Physics, Institute of Theoretical Physics,*
Chinese Academy of Sciences, Beijing 100190, China
[2]*Kobayashi-Maskawa Institute for the Origin of Particles and the Universe, Nagoya University,*
Nagoya 464–8602, Japan
[3]*Department of Physics, Florida State University, Tallahassee, Florida 32306, USA*
[4]*KEK Theory Center, IPNS, KEK, Tsukuba 305–0801, Japan*

A modified neutrino sector could imprint a signature on precision measurements of the quark sector because many such measurements rely on the semileptonic decays of the charged currents. Currently, global fits of the determinations of the Cabibbo-Kobayashi-Maskawa (CKM) matrix elements point to a 3σ-level deficit in the first-row CKM unitarity test, commonly referred to as the Cabibbo-angle anomaly. We find that a MeV sterile neutrino that mixes with the electron-type neutrino increases the extracted $|V_{ud}|$, accommodating the Cabibbo-angle anomaly. This MeV sterile neutrino affects the superallowed nuclear β decays and neutron decay, but it barely modifies the other measurements of the CKM elements. While various constraints may apply to such a sterile neutrino, we present viable scenarios within an extension of the inverse seesaw model.

DOI: 10.1103/PhysRevD.108.115034

I. INTRODUCTION

While precision measurements have largely confirmed the predictions of the standard model (SM), there are now unignorable deviations. Notably, certain observables, such as the lepton flavor universality in meson decays [1], have begun to diverge from SM predictions. Against this backdrop, the neutrino sector, often considered a relatively unexplored domain in direct determinations, offers intriguing possibilities. Many of these anomalies seemingly in the quark sector could be actually due to new physics (NP) of the neutrino sector, given that the relevant measurements heavily rely on the semileptonic decays involving neutrinos.

In this paper, we consider, as one such example, the unitarity relation of the Cabibbo-Kobayashi-Maskawa (CKM) matrix $VV^{\dagger} = I_3$ [2,3]. A deficit has been observed in the first-row CKM unitarity test [4–17]. According to a recent review in Ref. [16], we obtain

$$(VV^{\dagger})_{11} \equiv |V_{ud}|^2 + |V_{us}|^2 + |V_{ub}|^2 = 1 + \Delta_{\text{CKM}}^{\text{global}}, \quad (1)$$

*teppeik@itp.ac.cn
†ktobioka@fsu.edu

with

$$\Delta_{\text{CKM}}^{\text{global}} = \begin{cases} -1.51(53) \times 10^{-3} & (\text{w/bottle UCN best}), \\ -2.34(62) \times 10^{-3} & (\text{w/in-beam best}), \end{cases} \quad (2)$$

which deviate from the unitarity relation ($\Delta_{\text{CKM}}^{\text{global}} = 0$) at a significance of -2.8σ and -3.8σ, respectively. Here, all available data from the kaon, pion, tau lepton, hyperon decays, and various types of β decays are used in the global fit [16], and all the decays involve neutrinos. The difference in Eq. (2) comes from the two different input data of the neutron decays:

$$|V_{ud,n}| = 0.97413(43) \quad (\text{bottle UCN best}), \quad (3)$$

based on the single most precise bottle ultracold neutron (UCN) lifetime data $\tau_n^{\text{bottle}} = 877.75(36)$ sec [18], while

$$|V_{ud,n}| = 0.96866(131) \quad (\text{in-beam best}), \quad (4)$$

based on the in-beam one $\tau_n^{\text{beam}} = 887.7(2.2)$ sec [19]. Here, the single most precise data of the nucleon isovector axial charge g_A/g_V [20] and an updated radiative correction Δ_R [15] are used in both cases. It is found that the beam neutron data provides a little bit larger significance in the deficit. Note that as discussed in the following, $|V_{ud}|$ is mostly determined by the data of the superallowed nuclear β decays.

Since the size of $|V_{ub}|^2$ is significantly smaller than uncertainties of the other components [21,22], the deficit is essentially inherent in the two-generation Cabibbo angle. Hence, it is referred to as the *Cabibbo angle anomaly* (CAA) [6,7]. On the other hand, the ordinary CKM unitarity triangle (in B-meson decays) corresponds to $(V^\dagger V)_{31} = 0$, which is currently consistent with the SM prediction within the experimental errors [22]. The representative measurements specific to the $(VV^\dagger)_{11}$ unitarity test are: the superallowed nuclear β decay and the neutron decay for $|V_{ud}|$; the kaon decays such as $K \to \pi\ell\nu$, $K \to \mu\nu$, and tau hadronic decays for $|V_{us}|$ and their ratio $|V_{us}/V_{ud}|$. The recent global fit of them and assessment of the deficit of $(VV^\dagger)_{11}$ have been performed in Refs. [15,16].

There have been several attempts to resolve this anomaly by TeV-scale new physics models [5,7,8,10–17,23–35]. In this article, we develop deeper the extensions of neutrino sector concerning the anomaly. Our findings uniquely suggest that the CAA might be pointing to an intermediate mass scale for new particles, specifically, a sterile neutrino at the MeV scale that mixes with the electron-type neutrino [36,37]. This scenario could arise because all the relevant precision measurements use (semi)leptonic decays and involve neutrinos, considering that theoretical and experimental uncertainties of these decays are well managed. As we will show, the MeV sterile neutrino could be the underlying cause of the anomaly seemingly in the quark sector quantities. It is worth noting that several studies have indicated that the CAA is not easily resolved by heavy or massless sterile neutrinos [7,26,35].

In the next section, we delve into the contributions of sterile neutrinos to the observables for the CAA. In Sec. III, we summarize and discuss the current constraints on the favored parameter region, and conclude in Sec. IV.

II. STERILE NEUTRINO IN LIGHT OF CAA

This section outlines how a sterile neutrino might resolve the CAA. We initially examine two simple limits: very heavy and massless sterile neutrinos and show that they cannot accommodate the CAA. On the other hand, a MeV-scale sterile neutrino presents a potential solution by influencing the $|V_{ud}|$ determinations. To ascertain this solution, we conduct global fits in search of the optimal parameter space. (Discussions on experimental constraints and underlying models will be presented in Sec. III.)

Typically, a sterile neutrino's characteristics in most models can be effectively captured by its mass, $m_{\nu4}$, and its mixing angles with the SM neutrinos, $U_{\ell4}$. Below the electroweak scale, the SM neutrinos from the weak doublets, ν_ℓ, split into two pieces in the mass eigenbasis,

$$\nu_\ell \simeq \cos U_{\ell4}\nu'_\ell + \sin U_{\ell4}\nu_4 \quad \text{for } \ell = e, \mu, \tau, \quad (5)$$
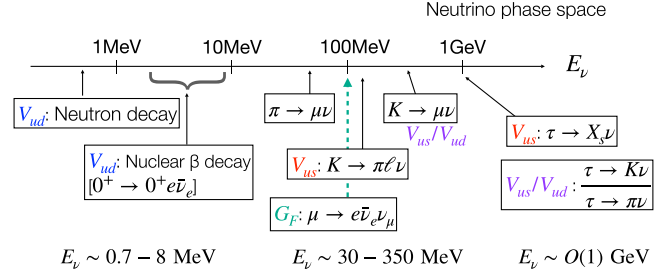

FIG. 1. Neutrino energy E_ν of each channel relevant to the first-row CKM unitarity test is summarized. The sterile neutrino channel is open when $m_{\nu4} < E_\nu$.

where ν'_ℓ are the SM-like neutrinos, often called active neutrinos. For the active neutrinos, the mixing ($\cos U_{\ell4} \lesssim 1$) results in the coupling reduction of the weak interaction, and the deficit gives the sterile neutrino a feeble coupling ($\sin U_{\ell4} \ll 1$) to the SM. These couplings alter observables primarily governed by the weak interaction, i.e., all the measurements relevant to the CAA are potentially affected, see Fig. 1. The sign of the modification depends on the mass scale of the sterile neutrino, pinpointing a specific scale.

A. Sterile neutrino above GeV

If the sterile neutrino mass exceeds $\mathcal{O}(1)$ GeV, it would not be kinematically permissible in the relevant measurements. In this case, an important modification occurs in the Fermi constant measurement via the muon decay. The observed value, G_F^{obs}, deviates from the true value, G_F, as described by

$$G_F^{\text{obs}} = G_F \cos U_{e4} \cos U_{\mu4}. \quad (6)$$

This relationship is pivotal in all the measurements employed in the CKM determinations. The CKM element V_{ud} is obtained by the superallowed nuclear β decay and neutron decay associated with ν'_e, and we have $V_{ud}^{\text{obs}} G_F^{\text{obs}} = V_{ud} G_F \cos U_{e4}$ which leads to

$$V_{ud}^{\text{obs}} = V_{ud}/\cos U_{\mu4}. \quad (7)$$

Other elements V_{us} and its ratio V_{us}/V_{ud} are derived from the measurements involving ν'_μ.[1] Analogous to Eq. (7), the relationships between the observed and true values are given by

$$V_{us}^{\text{obs}} = V_{us}/\cos U_{e4}, \quad (8)$$

$$(V_{us}/V_{ud})^{\text{obs}} = V_{us}/V_{ud}. \quad (9)$$

---

[1] V_{us} is also determined from the electron mode, $K \to \pi e\nu_e$ (with better precision than the muon mode), which leads to $V_{us}^{\text{obs}} = V_{us}/\cos U_{\mu4}$. But, combining Eq. (7), $\Delta_{\text{CKM}} > 0$ is predicted in either way.

Now one can check the unitarity relation, for example, combining Eq. (7) with (8),

$$1 + \Delta_{\text{CKM}} = |V_{ud}^{\text{obs}}|^2 + |V_{us}^{\text{obs}}|^2 = \frac{|V_{ud}|^2}{\cos^2 U_{\mu 4}} + \frac{|V_{us}|^2}{\cos^2 U_{e4}}. \quad (10)$$

Given the inherent CKM unitarity, represented by $|V_{ud}|^2 + |V_{us}|^2 \simeq 1$, it follows $\Delta_{\text{CKM}} > 0$, which is in contrast to the experimental fits presented in Eq. (2).[2] Similarly, combining Eqs. (7) and (9) draws the same conclusion.

B. Light sterile neutrino

Given that a heavy sterile neutrino cannot address the anomaly, it is instructive to examine the opposite scenario where the sterile neutrino mass is significantly smaller than E_ν, the maximum energy of neutrino in the relevant processes. Intriguingly, under these conditions, experimental observations align with the SM predictions. This is because the processes involving ν_4 are kinematically allowed and must be summed incoherently. To illustrate, consider the muon decay where we account for four processes,

$$\sum_{\nu_i = \nu'_\mu, \nu_4, \bar{\nu}_j = \bar{\nu}'_e, \bar{\nu}_4} \Gamma(\mu \to e \nu_i \bar{\nu}_j)$$
$$\simeq (\cos^2 U_{e4} + \sin^2 U_{e4})(\cos^2 U_{\mu 4} + \sin^2 U_{\mu 4}) \Gamma_{\text{SM}}$$
$$= \Gamma_{\text{SM}}. \quad (11)$$

Similarly, other processes reproduce the SM predictions. Hence, Δ_{CKM} is expected to be zero, which is again incompatible with the current data.

C. MeV sterile neutrino interacting with electron

The above discussion tells the CAA may suggest an intermediate mass scale of the sterile neutrino. If the mass is in the MeV scale, the coupling reduction of the weak interaction remains in the neutron/nuclear decays, while other observables, especially the Fermi constant, stay almost the same as in the SM as seen in the Eq. (11). Consequently, only V_{ud} is modified,

$$V_{ud}^{\text{obs}} = V_{ud} \cos U_{e4}. \quad (12)$$

The other quantities, G_F^{obs}, V_{us}^{obs}, and $(V_{us}/V_{ud})^{\text{obs}}$, are the same as the SM ones because the corresponding E_ν is much larger than MeV. This realizes the experimentally favored value,

$$1 + \Delta_{\text{CKM}} = |V_{ud}|^2 \cos^2 U_{e4} + |V_{us}|^2 < 1. \quad (13)$$

From the size of the anomaly $\Delta_{\text{CKM}} \approx 10^{-3}$, we can infer that the favored mixing-angle-squared is $U_{e4}^2 \approx 10^{-3}$, and $U_{\mu 4}^2$ is not necessary.[3]

The sterile neutrino mass can be in the same order of E_ν of the neutron/nuclear decays relevant to V_{ud} measurements. In the following, we evaluate the sterile mass dependence in the neutron and nuclear decays, and we focus on the mixing with the electron neutrino.

1. Superallowed nuclear β decay

The measurements of V_{ud} in nuclear physics have been conducted through so-called superallowed $0^+ \to 0^+$ nuclear β decay, and the latest survey was given by Ref. [39]. A heavy nucleus of $J^P = 0^+$ decay to another nucleus of 0^+ with a significant wave function overlap (*superallowed*), emitting $e^+ \nu_e$ (β^+ decay). Also, only the vector current of the quark weak interaction can contribute (Fermi decay). There are 15 transitions utilized to determine $|V_{ud}|$ [39], and the released energy in these transitions varies according to the specific process. Note that the determination of V_{ud} is significantly dominated by a single transition, $^{26m}\text{Al} \to ^{26}\text{Mg}$ [40,41]. While a sterile neutrino might be absent in some processes, it could emerge in others with larger released energy, and the effect is suppressed by the phase space as well as the small mixing angle $\sin^2 U_{e4}$.

Let us explore how V_{ud} is measured and the impact of the massive sterile neutrino. The decay width for both the active and sterile neutrinos is given by

$$\frac{d\Gamma_{0^+}}{dE_e} = \left(\frac{\sqrt{E_e^2 - m_e^2} \sqrt{E_\nu^2 - m_\nu^2} E_e E_\nu}{16\pi^3} \right) \frac{|\mathcal{M}|^2}{E_e E_\nu M M'}, \quad (14)$$

where the parenthesis comes from the phase space calculation. The outgoing neutrino (positron) energy is $E_{\nu(e)}$, and $M(M')$ is the mass of the parent (daughter) nucleus. δM denotes the nucleus mass difference, which is $\delta M \equiv M - M' = Q_{\text{EC}} - m_e$ neglecting the electron binding energy of $\mathcal{O}(10)$ eV [42]. The electron-capture (EC) Q-value Q_{EC} is the experimentally measured quantity summarized in Table I of Ref. [39]. For example, $Q_{\text{EC}}(^{26m}\text{Al} \to ^{26}\text{Mg}) = 4.23$ MeV. The nucleus recoil energy E_{recoil} can be ignored because it is much smaller than the typical electron and nuclear energy. Thus the energy conservation is approximately held as $\delta M \simeq E_\nu + E_e$, leading to $m_e \leq E_e \leq \delta M - m_\nu$. This approximation greatly simplifies the calculation, and is valid until the precision

---

becomes as good as $\delta M/M \sim 10^{-4}$. With this accuracy, the matrix element is given by

$$|\mathcal{M}|^2 \simeq C E_e E_\nu M^2 G_F^2 |V_{ud}|^2, \quad (15)$$

where C is a numerical coefficient. Normally, one can extract the combination of $G_F^2 |V_{ud}|^2$ based on the $\mathcal{F}t$ values of each nuclear β decay, which will be described later, under the assumption that the neutrinos are massless.

We present a simple formalism to account for the modification due to the massive sterile neutrino. Given the mass of neutrino barely modifies the matrix element of Eq. (15), the massive neutrino effect appears through the phase space. We define the modified phase space integral as

$$I(m_\nu, \delta M) \equiv \int_{m_e}^{\delta M - m_\nu} dE_e \sqrt{E_e^2 - m_e^2} \sqrt{E_\nu^2 - m_\nu^2} E_e E_\nu, \quad (16)$$

where $I(0, \delta M)$ corresponds to the SM case (maximizes for a given δM), and the kinematically forbidden neutrino yields $I(m_\nu > \delta M - m_e, \delta M) = 0$. A single decay mode is given by the sum of the active and sterile neutrino channels. To extract the modification factor depending on the sterile neutrino mass and mixing angle, we normalize the decay width by the one with $m_{\nu 4} = 0$,

$$\frac{\Gamma_{0^+}}{\Gamma_{0^+, m_{\nu 4} = 0}} = \cos^2 U_{e4} + \frac{I(m_{\nu 4}, \delta M)}{I(0, \delta M)} \sin^2 U_{e4} \quad (17)$$

$$= 1 - \epsilon(m_{\nu 4}, \delta M) \sin^2 U_{e4}, \quad (18)$$

with

$$\epsilon(m_{\nu 4}, \delta M) \equiv 1 - \frac{I(m_{\nu 4}, \delta M)}{I(0, \delta M)}, \quad (19)$$

where $m_{\nu 4}$ represents the sterile neutrino mass. We found that Eq. (17) is consistent with a result of Ref. [36]. In Fig. 2, the phase space modification factor $\epsilon(m_{\nu 4}, \delta M)$ is plotted for each superallowed channel. There, the charge repulsion or attraction effect is included in accordance with Ref. [43], which has little impact. The measured $|V_{ud, 0^+}^{obs}|$ through the nuclear β decay is different from the value in the presence of the MeV sterile neutrino, and, therefore, we obtain

$$\Gamma_{0^+}^{obs} \propto |V_{ud, 0^+}^{obs}|^2 = [1 - \epsilon(m_{\nu 4}, \delta M) \sin^2 U_{e4}] |V_{ud, 0^+}|^2 \quad (20)$$

by using Eq. (18). This reproduces the concise expression of Eq. (12) when $m_{\nu 4} > \delta M - m_e$, corresponding to $\epsilon = 1$. Thus, we expect $U_{e4}^2 \approx \Delta_{CKM}^{global} \approx 10^{-3}$ to accommodate the CAA.
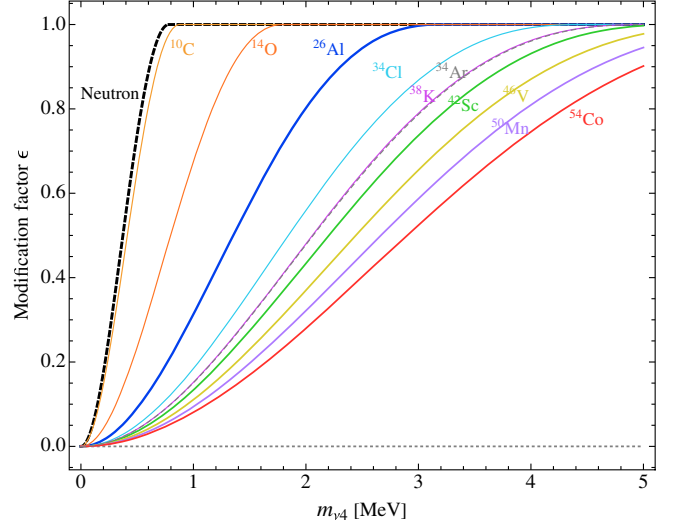

FIG. 2. The phase space modification factors $\epsilon(m_{\nu 4}, \delta M)$ are shown for the ten most accurate superallowed decays (solid lines and a dotted line) and the neutron decay (black dashed line).

2. Neutron decay

The neutron decay is currently the second-best probe of V_{ud}. The neutron lifetime (τ_n) measurements and the theoretical calculations are put together to obtain $V_{ud,n}$. It is known that there are two different measurements for the neutron lifetime, so-called neutron decays in the bottle or in the beam, and these data indicate $\approx 4\sigma$ discrepancy [44]. Although they are controversial, both results imply the violation of CKM unitarity, see details in the Introduction. In our fit, we treat two methods separately and combine it with other measurements. The sensitivity for V_{ud} is still dominated by the superallowed nuclear decay, but the favored sterile neutrino mass changes a little depending on the method of neutron lifetime measurements.

The effect of massive sterile neutrino is very similar to the case of superallowed nuclear decay. The neutron decay width is given by

$$\frac{\Gamma_n}{\Gamma_{n, m_{\nu 4} = 0}} = 1 - \epsilon(m_{\nu 4}, \delta M_{np}) \sin^2 U_{e4}, \quad (21)$$

where δM_{np} is the mass difference between a neutron and a proton. Hence, the observed $V_{ud,n}^{obs}$ can be smaller than the true value,

$$|V_{ud,n}^{obs}|^2 = [1 - \epsilon(m_{\nu 4}, \delta M_{np}) \sin^2 U_{e4}] |V_{ud,n}|^2. \quad (22)$$

The phase space modification factor $\epsilon(m_{\nu 4}, \delta M_{np})$ is shown in Fig. 2.

As we already addressed, the neutron lifetime measurements are mutually inconsistent between the bottle UCN and the beam methods. In this article, we treat them separately rather than combining.

3. Statistical combinations

Basically we construct χ^2 functions of $m_{\nu 4}$, $\sin^2 U_{e4} \simeq U_{e4}^2$, $|V_{ud}|$, and $|V_{us}|$, and impose the unitarity at the truth level, $|V_{ud}|^2 + |V_{us}|^2 = 1$, safely dropping $|V_{ub}|^2 \simeq 1.4 \times 10^{-5}$ for the uncertainty of Δ_{CKM} [21,22]. Also, we do not include the pion β decay $\pi^+ \to \pi^0 e^+ \nu$, which can independently measure V_{ud} without nuclear corrections, in our analysis, because its current sensitivity is approximately ten times weaker than that of superallowed β decay [15]. In this subsection, we omit the absolute value notation for simplicity.

We combine the V_{ud} measurements which depend on the sterile neutrino mass less than 10 MeV and the mixing, with V_{us} and V_{us}/V_{ud} measurements which have negligible shifts from the sterile neutrino, since $U_{e4}^2(m_{\nu 4}/E_\nu) \lesssim 10^{-4}$. We adopt the following fitted values: V_{us} from the semileptonic kaon decays ($K_{\ell 3}$), inclusive-hadronic τ decays, and hyperon semileptonic decays, and V_{us}/V_{ud} from the leptonic kaon-decay rate over the pion one ($K_{\mu 2}/\pi_{\mu 2}$) [16]

$$V_{us,\text{fit}} = 0.223\,14(51), \tag{23}$$

$$(V_{us}/V_{ud})_{\text{fit}} = 0.231\,08(51). \tag{24}$$

Then, we construct two χ^2 functions,

$$\chi_{us}^2(V_{ud}) = \frac{\left(\sqrt{1 - V_{ud}^2} - V_{us,\text{fit}}\right)^2}{(\delta V_{us})^2}, \tag{25}$$

$$\chi_{us/ud}^2(V_{ud}) = \frac{\left[\sqrt{1 - V_{ud}^2}/V_{ud} - (V_{us}/V_{ud})_{\text{fit}}\right]^2}{[\delta(V_{us}/V_{ud})]^2}, \tag{26}$$

where δV_{us} represents the uncertainty of $V_{us,\text{fit}}$, and so does $\delta(V_{us}/V_{ud})$.

For the V_{ud} determination through the neutron lifetime, we have to consider the effect of massive sterile neutrino, and then we have

$$\chi_n^2(m_{\nu 4}, U_{e4}^2, V_{ud}) = \frac{\left[V_{ud}\sqrt{1 - \epsilon(m_{\nu 4}, \delta M_{np})U_{e4}^2} - V_{ud,n}\right]^2}{(\delta V_{ud,n})^2}. \tag{27}$$

We have two different χ_n^2 functions for the $V_{ud,n} = 0.97413(43)$ at the bottle UCN experiment (3) and $V_{ud,n} = 0.96866(131)$ in the beam (4). We do not combine them due to their disagreement.

Next, we construct χ^2 function for the superallowed $0^+ \to 0^+$ nuclear β decay, where the ten most accurate nuclei data are used. Each superallowed transition is characterized by its own ft value, where f is a dimensionless constant that comes from an integral over phase space

and t is the half-lifetime of the $0^+ \to 0^+$ transition [45–47]. By subtracting the nuclear structure-dependent corrections from each ft value, one can obtain each corrected $\mathcal{F}t$ value, which is a nucleus-independent quantity according to the conserved vector current hypothesis, and sensitive to $(G_F^{\text{obs}} V_{ud}^{\text{obs}})^{-2}$. In the fit of ten superallowed nuclear decays, one needs a common nuisance parameter α to account for the total systematic uncertainty. With this consideration, χ^2 functions from the superallowed transitions are given by

$$
\begin{aligned}
&\chi_{0^+}^2(m_{\nu 4}, U_{e4}^2, V_{ud}, \alpha) \\
&= \sum_i \left(\mathcal{F}t_i - \frac{K(1 + \Delta_R^V)^{-1}(1 + \alpha)}{2G_F^2 V_{ud}^2[1 - \epsilon(m_{\nu 4}, \delta M_i)U_{e4}^2]}\right)^2 / (\delta \mathcal{F}t_i)^2,
\end{aligned}
\tag{28}
$$

$$\chi_{\text{sys}}^2(\alpha) = \frac{\alpha^2}{\sigma_{\Delta_R^V}^2 + \sigma_{\delta_R'}^2 + \sigma_{\delta_{\text{NS}}}^2}, \tag{29}$$

where $G_F = 1.1663788(6) \times 10^{-5}$ GeV^{-2}, $K = 8120.27648(26) \times 10^{-10}$ GeV^{-4} s, and the index i runs ^{10}C, ^{14}O, ^{26m}Al, ^{34}Cl, ^{34}Ar, ^{38m}K, ^{42}Sc, ^{46}V, ^{50}Mn, and ^{54}Co, shown in Fig. 2. We use the transition-independent radiative correction $\Delta_R^V = 2.467(27) \times 10^{-2}$ from Eq. (A.8) of Ref. [15], giving $\sigma_{\Delta_R^V} = \delta\Delta_R^V/(1 + \Delta_R^V) = 2.63 \times 10^{-4}$. $\mathcal{F}t_i$ values are obtained from Table XVI of Ref. [39]. We extract $\sigma_{\delta_R'} = 0.36$ s$/3072$ s $= 1.17 \times 10^{-4}$ and $\sigma_{\delta_{\text{NS}}} = 1.73$ s$/3072$ s $= 5.63 \times 10^{-4}$ from Eq. (22) of Ref. [39].

For a crosscheck of our statistical scheme of the superallowed nuclear decays, when a sterile neutrino decoupling limit ($U_{e4} \to 0$ or $m_{\nu 4} \to 0$) is examined with $\Delta_R^V = 2.454(19) \times 10^{-2}$ given in Ref. [39], we obtained $V_{ud,0^+} = 0.97369(32)$, which well agrees with $V_{ud,0^+} = 0.97373(31)$ of Ref. [39].

Finally, we combine all the χ^2 functions using only one neutron χ^2 at a time,

$$\chi^2(m_{\nu 4}, U_{e4}^2, V_{ud}, \alpha) = \chi_{us}^2 + \chi_{us/ud}^2 + \chi_n^2 + \chi_{0^+}^2 + \chi_{\text{sys}}^2. \tag{30}$$

We find the global minimum $\chi_{\min}^2$ and search for the favored parameter space of the sterile neutrino by evaluating

$$\Delta\chi^2 \equiv \chi^2(m_{\nu 4}, U_{e4}^2, V_{ud}, \alpha) - \chi_{\min}^2, \tag{31}$$

where V_{ud}, as well as α, is treated as the nuisance parameters and thus minimized for a given set of $(m_{\nu 4}, U_{e4}^2)$.

The results are shown in Fig. 3. As expected, the favored mixing angle squared is $U_{e4}^2 \approx 10^{-3}$, and there is a plateau once the sterile neutrino mass $m_{\nu 4}$ is heavier than $\delta M - m_e \approx 3.2$ MeV, which is the maximum neutrino energy at the superallowed nuclear decay ^{26m}Al $\to$ ^{26}Mg, see also Fig. 2.
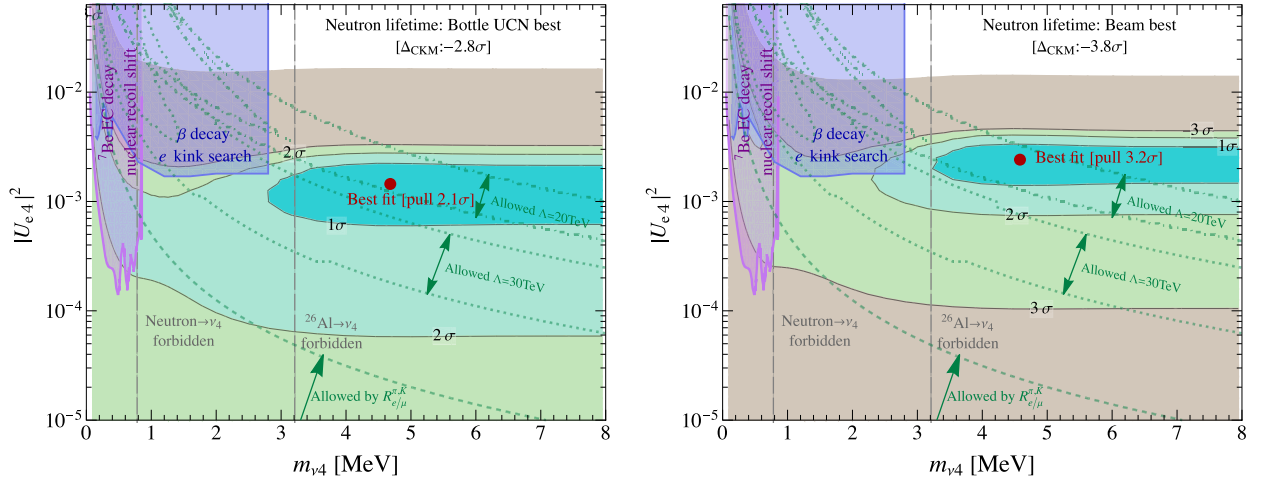
FIG. 3.   Favored parameter regions are shown. The red points represent the best-fit point with the pulls from the SM hypothesis. For the neutron decay data, the most precise neutron lifetime results from the bottle UCN and the beam measurements are used in the left and right panels, respectively. The blue and purple shaded regions are excluded by the nuclear β-decay kink searches [48–51] and the EC-decay search [52], respectively. The regions above green dashed lines can be constrained by $\pi^+ \to e^+\nu$ measurements [36,53,54], and the regions between dotted or dash-dotted green lines are allowed with the dimension-six operator. See more details in the text.

We show two panels depending on the neutron lifetime measurements. In the left panel, we use the bottle measurement to extract V_{ud}, which is consistent with the one from the superallowed nuclear decays. The original tension of the CAA is at 2.8σ, and the pull in the presence of sterile neutrino is 2.1σ at the best-fit point. On the other hand, since the beam measurement prefers smaller V_{ud} than the superallowed nuclear decays, a significance of the CAA is enhanced to be 3.8σ, and the sterile neutrino can relax it by 3.2σ at the best-fit point.

III. CONSTRAINTS OF MeV STERILE NEUTRINO

In the previous section, we identified the favored ranges of the mass and mixing of the sterile neutrino for the given anomaly. However, these parameter regions are subject to constraints from the laboratory to the cosmology. In this section, we list all the relevant bounds and show consistent resolutions if exist.

A. Direct bounds

There have been kink searches in the Kurie plot, the emitted electron energy spectrum measurements in the nuclear β decays, to test the mass of sterile neutrino [48–51]. One relevant measurement is the kink search in ^{20}F decay which covers $m_{\nu 4} \lesssim 3$ MeV [49]. The blue-shaded regions in Fig. 3 are excluded by the kink searches. This is a robust bound on the sterile neutrino.

Furthermore, recently the BeEST experiment has set a constraint on the sterile neutrino through the EC-β decay using the superconducting quantum sensor [52]. This bound is shown by the purple-shaded regions in Fig. 3, which significantly improved the bound on the sterile

neutrino mixing U_{e4} with $m_{\nu 4} = 0.1$ MeV–0.8 MeV. This bound is also robust in our scenario.

B. $0\nu\beta\beta$ bound

Searches for the neutrinoless double beta decay ($0\nu\beta\beta$) are sensitive to Majorana neutrino mass and mixing. See the recent review [51,55]. If a $3+1$ sterile neutrino scenario (three active neutrinos plus one Majorana sterile neutrino) is considered, the $0\nu\beta\beta$ rate is proportional to $|U_{e4}^2 m_{\nu 4}|^2$. In this simplest case, the current measurements [56,57] set the upper limit on $U_{e4}^2 < 10^{-7}$ at $m_{\nu 4} = \mathcal{O}(1)$ MeV [51], which excludes the whole parameter region of Fig. 3.

However, it is known that the $0\nu\beta\beta$ bound can be suppressed by a generalized $B-L$ symmetry [58]. In particular, the bound is totally suppressed within the inverse seesaw model [59–61] in this category. In this scenario, the left-handed singlet fermion S as well as the right-handed neutrino N are introduced to the SM Lagrangian [62],

$$-\mathcal{L} = \frac{1}{2}\bar{N}^c \mu_N N + y\bar{L}\tilde{H}N + \frac{1}{2}\bar{S}^c \mu_S S + \bar{S}M_N N + \text{H.c.,} \quad (32)$$

where μ_N and μ_S are Majorana masses, which are small lepton number violations and are technically natural. After taking the mass eigenbasis, the active neutrino mass is

$$m_{\nu_\ell} \simeq \frac{M_D^2}{M_N^2}\mu_S \simeq U_{e4}^2 \mu_S, \quad (33)$$

where the mixing is $U_{e4}^2 \simeq (M_D/M_N)^2$, while the sterile neutrino becomes a pseudo-Dirac fermion with mass as

$$m_{\nu 4} \simeq M_N \pm \frac{\mu_S}{2}. \quad (34)$$

Here, $M_N \gg M_D = vy$ ($v \simeq 174$ GeV) is assumed. Note that μ_N is an irrelevant parameter at the leading order.

The smallness of the active neutrino masses requires μ_S to be suppressed in the inverse seesaw model, namely $\mu_s \approx \mathcal{O}(1)$ eV in the parameter of our interest. Consequently, the $0\nu\beta\beta$ rate, which has to pick up the Majorana mass μ_s, is significantly smaller than in the $3+1$ scenario and contained well below the observed limit for $m_{\nu 4} \lesssim \mathcal{O}(100)$ MeV [51].

C. Meson decay bounds

The sterile neutrino bounds from meson leptonic decays have been discussed in Ref. [63]. Within the SM, $\pi^+ \rightarrow e^+\nu$ decay is helicity-suppressed by the electron mass ($m_e^2/m_{\pi^+}^2$). On the other hand, when the sterile neutrino is heavier than the electron, the branching ratio is significantly modified. Strong constraints come from the e-μ universality measurements in the two-body leptonic decays of π^+ and K^+ [63–68],

$$R_{e/\mu}^M = \frac{\mathrm{BR}(M^+ \rightarrow e^+\nu(\gamma))}{\mathrm{BR}(M^+ \rightarrow \mu^+\nu(\gamma))}, \quad \text{for } M = \pi, K. \quad (35)$$

In Fig. 3, the areas above the green dashed lines are excluded by the latest analysis of $R_{e/\mu}^\pi$ at the PiENu experiment [36,53,54] (the bound from $R_{e/\mu}^K$ is weaker [69]). In the minimal scenario of the sterile neutrino with the mass and mixing to the weak interaction, this bound excludes the significant part of the favored parameter space for the CAA.[4]

However, if there are some higher dimensional operators that contain the sterile neutrino and induce $\pi^+ \rightarrow e^+\nu_4$, they can reduce $\pi^+ \rightarrow e^+\nu_4$ while keeping the nuclear and neutron β decay unaffected. This is because the SM-like amplitude of the pion decay is actually suppressed by the lepton mass, so its electron mode is sensitive to new physics contributions. Even with new physics of $\mathcal{O}(10)$ TeV scale, the $R_{e/\mu}^\pi$ bound can be easily compensated by small modification due to the higher dimensional operators.

For example, $R_{e/\mu}^M$ is sensitive to a dimension-six scalar operator $(\bar{u}_R V_{ui} d_L^i)(\bar{e}_L N)$, which can destructively interfere with the mixing contribution of Eq. (5), and we introduce

$$\mathcal{L}_{\mathrm{eff}} = \frac{1}{\Lambda^2}[\bar{u}_R(V_{ud}d_L + V_{us}s_L)](\bar{e}_L N) + \mathrm{H.c.}. \quad (36)$$

In Fig. 3, we show that modified allowed regions of $R_{e/\mu}^M$ for the cases of $\Lambda = 20$ TeV and 30 TeV by the green

---

[4]The introduction of the muon-neutrino mixing ($U_{\mu 4}$) does not ameliorate the situation. It is because the effect to $R_{e/\mu}^M$ from U_{e4}^2 is chirality enhanced by a factor of $m_{\nu 4}^2/m_e^2$. In contrast, the effect from $U_{\mu 4}^2$ is diminished, being suppressed by $m_{\nu 4}^2/m_M^2$ for $M = \pi$, K [36].

dash-dotted and dotted lines, respectively. It is found that the $R_{e/\mu}^M$ bound is significantly sensitive to the operator of Eq. (36), and the CAA favors the dimension-six operator with $\Lambda = 20$–30 TeV.

D. Long-lived sterile neutrino and cosmology

When the sterile neutrino lifetime is determined by the weak decay, the reactor [70,71] and Borexino experiments [72] use $\nu_4 \rightarrow e^+e^-\nu_e'$ decay mode to probe the range of 1 MeV $< m_{\nu 4} < 14$ MeV [51]. These bounds potentially exclude the favored regions of Fig. 3. However, the bounds are not applied if the lifetime is shorter by a factor of $\mathcal{O}(10$–$100)$ due to the additional decay modes.

The decay of sterile neutrino to three active neutrinos becomes significant in the presence of a real scalar mediator ϕ described by

$$-\mathcal{L} = \frac{m_\phi^2}{2}\phi^2 + \left(\frac{\lambda}{2}\phi\bar{S}^c S + \mathrm{H.c.}\right). \quad (37)$$

If the effective interaction scale satisfies $\lambda^2/m_\phi^2 \gtrsim 10U_{e4}^{-2}G_F \sim 0.1/\mathrm{GeV}^2$, the decay of the sterile neutrino is short enough. We find, when $m_\phi \simeq 0.5$ GeV–30 GeV, this condition is compatible with the bounds, such as the meson decays, studied in Ref. [73] since the mediator interactions with the active-neutrino are suppressed by the mixing angle as $\frac{1}{2}\lambda U_{e4}^2\phi\bar{\nu}_e^c\nu_e$, $\lambda U_{e4}\phi\bar{S}^c\nu_e$.

The cosmological observations typically constrain the MeV scale sterile neutrino. However, with the required mediator-interaction, the sterile neutrino decoupling from the SM thermal bath occurs together with the active neutrinos decoupling at $T \sim 2$ MeV. As a result, the remaining bound is from the effective number of neutrinos, N_{eff}. As the sterile neutrinos are not completely nonrelativistic at the decoupling temperature, they would increase the effective number of neutrinos by $\Delta N_{\mathrm{eff}} \simeq 1.0$–$0.25$ for $m_{\nu 4} = 5$–10 MeV. Although $\Delta N_{\mathrm{eff}} \gtrsim 0.3$ is constrained by the CMB observations [74], additional well-motivated particles, such as heavy axions with a lifetime of about 0.1–1 sec, can consistently compensate ΔN_{eff} [75,76].

In the absence of additional long-lived particles affecting N_{eff}, a different set of mediator interactions,

$$-\mathcal{L}_\phi = \frac{m_\phi^2}{2}\phi^2 + \frac{\phi}{4\Lambda_\gamma}F_{\mu\nu}F^{\mu\nu} + (\lambda'\phi\bar{S}_L N + \mathrm{H.c.}), \quad (38)$$

can lead to another consistent scenario. In this case, the sterile neutrino decay is predominantly $\nu_4 \rightarrow \phi^{(*)}\nu_e' \rightarrow \gamma\gamma\nu_e'$ which dismisses the reactor and Borexino bounds. The thermal history is modified such that the sterile neutrino interaction with the photons determines the decoupling from the thermal bath. The temperature when the entire neutrino sector decouples can be lower to 1(0.75) MeV,

which is about the temperature of neutron decoupling. The sterile neutrino at this temperature is nonrelativistic enough such that $\Delta N_{\text{eff}} \simeq 0.3$–$9 \times 10^{-3}(0.1$–$6 \times 10^{-4})$ for $m_{\nu 4} = 5$–10 MeV is allowed by the CMB. This scenario requires $\lambda'/(m_\phi^2)\Lambda \gtrsim 0.03/\text{GeV}^3$. Considering the bounds involving neutrino [73] and photon [77,78], we find that the mediator is allowed when $m_\phi \simeq 0.5$ GeV–4 GeV and $\lambda' \gtrsim 1$.

E. PMNS unitarity test

The Pontecorvo-Maki-Nakagawa-Sakata (PMNS) matrix [79,80] is a unitary matrix relating the mass eigenstates of neutrinos to the charged-lepton flavor eigenstates. Although the PMNS matrix is usually defined within three active neutrinos, the presence of sterile neutrinos extends the matrix and makes the 3×3 sub-matrix non-unitary. Hence, the unitarity test on the submatrix with consideration of neutrino oscillation data constraints the mixing elements due to the sterile neutrinos [81–85]. The recent global analysis suggests $|U_{e4}|^2 \lesssim 0.03$ at 2σ [85], which is sufficiently weaker than the size of $|U_{e4}|^2$ favored by the CAA within our scenario.

F. Summary of the constraints

Given the potential constraints for the parameter space favored by the CAA, the inverse seesaw models with a mediator ϕ and a higher dimensional operator emerge as viable scenarios. Even in the presence of the additional decay modes of the sterile neutrino via the mediator, it remains effectively stable in most laboratory experiments, in particular, measurements of neutron and nuclear β decays.

IV. CONCLUSIONS

Currently, it is reported that the first-row CKM unitarity test is violated at the 2.8σ level, referred to as the Cabibbo angle anomaly (CAA). This violation is worse when the neutron lifetime data of the in-beam experiment is used in the global fit. In this article, we point out that the MeV sterile neutrino that mixes the electron-type neutrino with $U_{e4}^2 \approx 10^{-3}$ can decrease the value of extracted $|V_{ud}^{\text{obs}}|$ from the superallowed nuclear β decays and the neutron decay relative to its true value, without modifying other observables relevant to the CKM determinations. As a result, it is found that the MeV sterile neutrino can alleviate the CAA. The parameter space of the sterile neutrino favored as the solution of the CAA is typically subject to various constraints. Although the nuclear β decay bounds are robust, we show that the sterile neutrino in the inverse seesaw models with the dimension-six operators can evade the laboratory constraints, and the neutrino mediator is favored by the cosmology bounds.

While we highlighted the sterile neutrino resolving the anomaly of the unitarity test, this type of scenario where new physics primarily in the neutrino sector gives apparent deviations in the precision measurements on the quark sector could be interesting in a broader context.

Note added. After completing this work, a new lattice calculation [86] reported $\Delta_R^V = 0.02439(19)$. If we adopt this result for the global fit of the superallowed nuclear β decays, significance of the tension is reduced by about 0.5σ, and correspondingly, the improvement of CAA (the pull with respect to the SM) due to the sterile neutrino is reduced by about 0.5σ.

[1] Heavy Flavor Averaging Group, HFLAV Collaboration, Averages of b-hadron, c-hadron, and τ-lepton properties as of 2021, Phys. Rev. D **107**, 052008 (2023).

[2] N. Cabibbo, Unitary symmetry and leptonic decays, Phys. Rev. Lett. **10**, 531 (1963).

[3] M. Kobayashi and T. Maskawa, *CP* violation in the renormalizable theory of weak interaction, Prog. Theor. Phys. **49**, 652 (1973).

[4] C.-Y. Seng, M. Gorchtein, H. H. Patel, and M. J. Ramsey-Musolf, Reduced hadronic uncertainty in the determination of V_{ud}, Phys. Rev. Lett. **121**, 241804 (2018).

[5] B. Belfatto, R. Beradze, and Z. Berezhiani, The CKM unitarity problem: A trace of new physics at the TeV scale? Eur. Phys. J. C **80**, 149 (2020).

[6] Y. Grossman, E. Passemar, and S. Schacht, On the statistical treatment of the Cabibbo angle anomaly, J. High Energy Phys. 07 (2020) 068.

[7] A. M. Coutinho, A. Crivellin, and C. A. Manzari, Global fit to modified neutrino couplings and the Cabibbo-angle anomaly, Phys. Rev. Lett. **125**, 071802 (2020).

[8] K. Cheung, W.-Y. Keung, C.-T. Lu, and P.-Y. Tseng, Vector-like quark interpretation for the CKM unitarity violation,

excess in Higgs signal strength, and bottom quark forward-backward asymmetry, J. High Energy Phys. 05 (2020) 117.

[9] C.-Y. Seng, X. Feng, M. Gorchtein, and L.-C. Jin, Joint lattice QCD–dispersion theory analysis confirms the quark-mixing top-row unitarity deficit, Phys. Rev. D **101,** 111301 (2020).

[10] A. Crivellin, F. Kirk, C. A. Manzari, and M. Montull, Global electroweak fit and vector-like leptons in light of the Cabibbo angle anomaly, J. High Energy Phys. 12 (2020) 166.

[11] M. Kirk, Cabibbo anomaly versus electroweak precision tests: An exploration of extensions of the standard model, Phys. Rev. D **103,** 035004 (2021).

[12] A. Crivellin, M. Hoferichter, and C. A. Manzari, Fermi constant from muon decay versus electroweak fits and Cabibbo-Kobayashi-Maskawa unitarity, Phys. Rev. Lett. **127,** 071801 (2021).

[13] B. Belfatto and Z. Berezhiani, Are the CKM anomalies induced by vector-like quarks? Limits from flavor changing and Standard Model precision tests, J. High Energy Phys. 10 (2021) 079.

[14] D. Bryman, V. Cirigliano, A. Crivellin, and G. Inguglia, Testing lepton flavor universality with pion, kaon, tau, and beta decays, Annu. Rev. Nucl. Part. Sci. **72,** 69 (2022).

[15] V. Cirigliano, A. Crivellin, M. Hoferichter, and M. Moulson, Scrutinizing CKM unitarity with a new measurement of the $K_{\mu3}/K_{\mu2}$ branching fraction, Phys. Lett. B **838,** 137748 (2023).

[16] A. Crivellin, M. Kirk, T. Kitahara, and F. Mescia, Global fit of modified quark couplings to EW gauge bosons and vector-like quarks in light of the Cabibbo angle anomaly, J. High Energy Phys. 03 (2023) 234.

[17] B. Belfatto and S. Trifinopoulos, The remarkable role of the vector-like quark doublet in the Cabibbo angle and W-mass anomalies, Phys. Rev. D **108,** 035022 (2023).

[18] UCNτ Collaboration, Improved neutron lifetime measurement with UCNτ, Phys. Rev. Lett. **127,** 162501 (2021).

[19] A. T. Yue, M. S. Dewey, D. M. Gilliam, G. L. Greene, A. B. Laptev, J. S. Nico, W. M. Snow, and F. E. Wietfeldt, Improved determination of the neutron lifetime, Phys. Rev. Lett. **111,** 222501 (2013).

[20] B. Märkisch *et al.*, Measurement of the weak axial-vector coupling constant in the decay of free neutrons using a pulsed cold neutron beam, Phys. Rev. Lett. **122,** 242501 (2019).

[21] CKMfitter Group Collaboration, *CP* violation and the CKM matrix: Assessing the impact of the asymmetric *B* factories, Eur. Phys. J. C **41,** 1 (2005).

[22] UTfit Collaboration, New UTfit analysis of the unitarity triangle in the Cabibbo-Kobayashi-Maskawa scheme, Rend. Lincei Sci. Fis. Nat. **34,** 37 (2023).

[23] A. Crivellin and M. Hoferichter, β decays as sensitive probes of lepton flavor universality, Phys. Rev. Lett. **125,** 111801 (2020).

[24] M. Endo and S. Mishima, Muon $g-2$ and CKM unitarity in extra lepton models, J. High Energy Phys. 08 (2020) 004.

[25] B. Capdevila, A. Crivellin, C. A. Manzari, and M. Montull, Explaining $b \to s\ell^+\ell^-$ and the Cabibbo angle anomaly with a vector triplet, Phys. Rev. D **103,** 015032 (2021).

[26] T. Li, X.-D. Ma, and M. A. Schmidt, Constraints on the charged currents in general neutrino interactions with sterile neutrinos, J. High Energy Phys. 10 (2020) 115.

[27] A. Crivellin, C. A. Manzari, M. Alguero, and J. Matias, Combined explanation of the $Z \to bb^-$ forward-backward asymmetry, the Cabibbo angle anomaly, and $\tau \to \mu\nu\nu$ and $b \to s\ell + \ell$- data, Phys. Rev. Lett. **127,** 011801 (2021).

[28] A. Crivellin, F. Kirk, C. A. Manzari, and L. Panizzi, Searching for lepton flavor universality violation and collider signals from a singly charged scalar singlet, Phys. Rev. D **103,** 073002 (2021).

[29] T. Felkl, J. Herrero-Garcia, and M. A. Schmidt, The singly-charged scalar singlet as the origin of neutrino masses, J. High Energy Phys. 05 (2021) 122; 05 (2022) 73.

[30] G. C. Branco, J. T. Penedo, P. M. F. Pereira, M. N. Rebelo, and J. I. Silva-Marcos, Addressing the CKM unitarity problem with a vector-like up quark, J. High Energy Phys. 07 (2021) 099.

[31] D. Marzocca and S. Trifinopoulos, Minimal explanation of flavor anomalies: B-meson decays, muon magnetic moment, and the Cabibbo angle, Phys. Rev. Lett. **127,** 061803 (2021).

[32] A. J. Buras, A. Crivellin, F. Kirk, C. A. Manzari, and M. Montull, Global analysis of leptophilic Z' bosons, J. High Energy Phys. 06 (2021) 068.

[33] A. Crivellin, M. Hoferichter, M. Kirk, C. A. Manzari, and L. Schnell, First-generation new physics in simplified models: From low-energy parity violation to the LHC, J. High Energy Phys. 10 (2021) 221.

[34] V. Cirigliano, D. Díaz-Calderón, A. Falkowski, M. González-Alonso, and A. Rodríguez-Sánchez, Semileptonic tau decays beyond the standard model, J. High Energy Phys. 04 (2022) 152.

[35] M. Blennow, P. Coloma, E. Fernández-Martínez, and M. González-López, Right-handed neutrinos and the CDF II anomaly, Phys. Rev. D **106,** 073005 (2022).

[36] D. A. Bryman and R. Shrock, Constraints on sterile neutrinos in the MeV to GeV mass range, Phys. Rev. D **100,** 073011 (2019).

[37] T. Kitahara and K. Tobioka, Sterile neutrinos in light of the Cabibbo-angle anomaly, J. Phys. Conf. Ser. **2446,** 012009 (2023).

[38] CDF Collaboration, High-precision measurement of the W boson mass with the CDF II detector, Science **376,** 170 (2022).

[39] J. C. Hardy and I. S. Towner, Superallowed $0^+ \to 0^+$ nuclear β decays: 2020 critical survey, with implications for V_{ud} and CKM unitarity, Phys. Rev. C **102,** 045501 (2020).

[40] S. A. Brindhaban and P. H. Barker, The Q value for the Alm26 superallowed beta decay, Phys. Rev. C **49,** 2401 (1994).

[41] T. Eronen *et al.*, Q-values of the superallowed beta-emitters Al-26-m, Sc-42 and V-46 and their impact on V(ud) and the unitarity of the CKM matrix, Phys. Rev. Lett. **97,** 232501 (2006).

[42] A. Kramida, Yu. Ralchenko, and J. Reader (NIST ASD Team), NIST Atomic Spectra Database (ver. 5.10), Available: https://www.nist.gov/pml/atomic-spectra-database, National Institute of Standards and Technology, Gaithersburg, MD., 2022.

[43] M. Kleesiek *et al.*, β-decay spectrum, response function and statistical model for neutrino mass measurements with the KATRIN experiment, Eur. Phys. J. C **79**, 204 (2019).

[44] A. Czarnecki, W. J. Marciano, and A. Sirlin, Neutron lifetime and axial coupling connection, Phys. Rev. Lett. **120**, 202002 (2018).

[45] J. C. Hardy and I. S. Towner, New limit on fundamental weak-interaction parameters from superallowed beta decay, Phys. Rev. Lett. **94**, 092502 (2005).

[46] J. C. Hardy and I. S. Towner, Superallowed $0^+ \to 0^+$ nuclear beta decays: A critical survey with tests of CVC and the standard model, Phys. Rev. C **71**, 055501 (2005).

[47] J. C. Hardy and I. S. Towner, Superallowed $0^+ \to 0^+$ nuclear beta decays: A new survey with precision tests of the conserved vector current hypothesis and the standard model, Phys. Rev. C **79**, 055502 (2009).

[48] K. Schreckenbach, G. Colvin, and F. Von Feilitzsch, Search for mixing of heavy neutrinos in the β^+ and β^- spectra of the ^{64}Cu decay, Phys. Lett. **129B**, 265 (1983).

[49] J. Deutsch, M. Lebrun, and R. Prieels, Searches for admixture of massive neutrinos into the electron flavor, Nucl. Phys. **A518**, 149 (1990).

[50] A. V. Derbin, I. S. Drachnev, I. S. Lomskaya, V. N. Muratova, N. V. Pilipenko, D. A. Semenov, L. M. Tukkhonen, E. V. Unzhakov, and A. Kh. Khusainov, Search for a neutrino with a mass of 0.01–1.0 MeV in beta decays of ^{144}Ce–^{144}Pr nuclei, JETP Lett. **108**, 499 (2018).

[51] P. D. Bolton, F. F. Deppisch, and P. S. Bhupal Dev, Neutrinoless double beta decay versus other probes of heavy sterile neutrinos, J. High Energy Phys. 03 (2020) 170.

[52] S. Friedrich *et al.*, Limits on the existence of sub-MeV sterile neutrinos from the decay of ^{7}Be in superconducting quantum sensors, Phys. Rev. Lett. **126**, 021803 (2021).

[53] PiENu Collaboration, Improved measurement of the $\pi \to e\nu$ branching ratio, Phys. Rev. Lett. **115**, 071801 (2015).

[54] D. A. Bryman and R. Shrock, Improved constraints on sterile neutrinos in the MeV to GeV mass range, Phys. Rev. D **100**, 053006 (2019).

[55] W. Dekens, J. de Vries, E. Mereghetti, J. Menéndez, P. Soriano, and G. Zhou, Neutrinoless double-beta decay in the neutrino-extended standard model, Phys. Rev. C **108**, 045501 (2023).

[56] KamLAND-Zen Collaboration, Search for Majorana neutrinos near the inverted mass hierarchy region with KamLAND-Zen, Phys. Rev. Lett. **117**, 082503 (2016). **117**, 109903(A) (2016).

[57] GERDA Collaboration, Improved limit on neutrinoless double-β decay of ^{76}Ge from GERDA phase II, Phys. Rev. Lett. **120**, 132503 (2018).

[58] M. Chrzaszcz, M. Drewes, T. E. Gonzalo, J. Harz, S. Krishnamurthy, and C. Weniger, A frequentist analysis of three right-handed neutrinos with GAMBIT, Eur. Phys. J. C **80**, 569 (2020).

[59] R. N. Mohapatra and J. W. F. Valle, Neutrino mass and baryon number nonconservation in superstring models, Phys. Rev. D **34**, 1642 (1986).

[60] R. N. Mohapatra, Mechanism for understanding small neutrino mass in superstring theories, Phys. Rev. Lett. **56**, 561 (1986).

[61] S. Nandi and U. Sarkar, A solution to the neutrino mass problem in superstring E6 theory, Phys. Rev. Lett. **56**, 564 (1986).

[62] P. S. Bhupal Dev and A. Pilaftsis, Light and superlight sterile neutrinos in the minimal radiative inverse seesaw model, Phys. Rev. D **87**, 053007 (2013).

[63] R. E. Shrock, General theory of weak leptonic and semileptonic decays. 1. Leptonic pseudoscalar meson decays, with associated tests for, and bounds on, neutrino masses and lepton mixing, Phys. Rev. D **24**, 1232 (1981).

[64] J. Tran Thanh Van, Search for massive neutrinos in $\pi \to \nu_e$ decay, Phys. Rev. Lett. **50**, 1546 (1983).

[65] D. I. Britton *et al.*, Measurement of the $\pi^+ \to e^+\nu$ branching ratio, Phys. Rev. Lett. **68**, 3000 (1992).

[66] D. I. Britton *et al.*, Improved search for massive neutrinos in $\pi^+ \to e^+\nu$ decay, Phys. Rev. D **46**, R885 (1992).

[67] A. Abada, D. Das, A. M. Teixeira, A. Vicente, and C. Weiland, Tree-level lepton universality violation in the presence of sterile neutrinos: Impact for R_K and R_π, J. High Energy Phys. 02 (2013) 048.

[68] A. Abada, A. M. Teixeira, A. Vicente, and C. Weiland, Sterile neutrinos in leptonic and semileptonic decays, J. High Energy Phys. 02 (2014) 091.

[69] NA62 Collaboration, Precision measurement of the ratio of the charged kaon leptonic decay rates, Phys. Lett. B **719**, 326 (2013).

[70] A. I. Derbin *et al.*, Experiment on anti-neutrino scattering by electrons at a reactor of the Rovno nuclear power plant, JETP Lett. **57**, 768 (1993).

[71] C. Hagner, M. Altmann, F. V. Feilitzsch, L. Oberauer, Y. Declais, and E. Kajfasz, Experimental search for the neutrino decay $\nu_3 \to \nu_j + e^+ + e^-$ and limits on neutrino mixing, Phys. Rev. D **52**, 1343 (1995).

[72] Borexino Collaboration, New limits on heavy sterile neutrino mixing in B8 decay obtained with the Borexino detector, Phys. Rev. D **88**, 072010 (2013).

[73] A. de Gouvêa, P. S. Bhupal Dev, B. Dutta, T. Ghosh, T. Han, and Y. Zhang, Leptonic scalars at the LHC, J. High Energy Phys. 07 (2020) 142.

[74] Planck Collaboration, Planck 2018 results. VI. Cosmological parameters, Astron. Astrophys. **641**, A6 (2020); **652**, C4 (E) (2021).

[75] D. Cadamuro, S. Hannestad, G. Raffelt, and J. Redondo, Cosmological bounds on sub-MeV mass axions, J. Cosmol. Astropart. Phys. 02 (2011) 003.

[76] D. I. Dunsky, L. J. Hall, and K. Harigaya, Dark radiation constraints on heavy QCD axions, arXiv:2205.11540.

[77] M. J. Dolan, T. Ferber, C. Hearty, F. Kahlhoefer, and K. Schmidt-Hoberg, Revised constraints and Belle II sensitivity for visible and invisible axion-like particles, J. High Energy Phys. 12 (2017) 094; 03 (2021) 190(E).

[78] S. Gori, G. Perez, and K. Tobioka, KOTO vs. NA62 dark scalar searches, J. High Energy Phys. 08 (2020) 110.

[79] B. Pontecorvo, Inverse beta processes and nonconservation of lepton charge, Zh. Eksp. Teor. Fiz. **34**, 247 (1957).

[80] Z. Maki, M. Nakagawa, and S. Sakata, Remarks on the unified model of elementary particles, Prog. Theor. Phys. **28**, 870 (1962).

[81] S. Parke and M. Ross-Lonergan, Unitarity and the three flavor neutrino mixing matrix, Phys. Rev. D **93,** 113009 (2016).

[82] C. S. Fong, H. Minakata, and H. Nunokawa, A framework for testing leptonic unitarity by neutrino oscillation experiments, J. High Energy Phys. 02 (2017) 114.

[83] S. A. R. Ellis, K. J. Kelly, and S. W. Li, Current and future neutrino oscillation constraints on leptonic unitarity, J. High Energy Phys. 12 (2020) 068.

[84] Z. Hu, J. Ling, J. Tang, and T. Wang, Global oscillation data analysis on the 3ν mixing without unitarity, J. High Energy Phys. 01 (2021) 124.

[85] K. Goldhagen, M. Maltoni, S. E. Reichard, and T. Schwetz, Testing sterile neutrino mixing with present and future solar neutrino data, Eur. Phys. J. C **82,** 116 (2022).

[86] P.-X. Ma *et al.*, Lattice QCD calculation of electroweak box contributions to superallowed nuclear and neutron beta decays, arXiv:2308.16755.